ACS APPLIED MATERIALS & INTERFACES

Research Article

www.acsami.org

Low-Temperature Growth of Bismuth Thin Films with (111) Facet on Highly Oriented Pyrolytic Graphite

Fei Song,*[,†,‡] Justin W. Wells,[‡] Zheng Jiang,[†] Magne Saxegaard,[‡] and Erik Wahlström*[,‡]

[†]Shanghai Institute of Applied Physics, Chinese Academy of Sciences, Shanghai, 201204, China

[‡]Department of Physics, Norwegian University of Science and Technology, N-7030, Trondheim, Norway

ABSTRACT: The epitaxial growth of artificial two-dimensional metals at interfaces plays a key role in fabricating heterostructures for nanoelectronics. Here, we present the growth of bismuth nanostructures on highly oriented pyrolytic graphite (HOPG) under ultrahigh vacuum (UHV) conditions, which was investigated thoroughly by a combination of scanning tunneling microscopy (STM), ultraviolet photoemission spectroscopy (UPS), X-ray photoelectron spectroscopy (XPS), and low energy electron diffraction (LEED). It was found that (111)-oriented bilayers are formed on as-cleaved high-quality HOPG at 140 K, which opens the possibility of making Bi(111) thin films on a semimetal, and this is a notable step forward from the earlier studies, which show that only Bi(110) facets could be formed at ultrathin thickness at room temperature. XPS investigation of both C 1s and Bi 4f reflects the rather weak bonding between the Bi film and the HOPG substrate and suggests a quasi layer-by-layer growth mode of Bi nanostructures on HOPG at low temperature. Moreover, the evolution of the valence band of the interface is recorded by UPS, and a transition from quantum well states to bulk-like features is observed at varying film thickness. Unlike semimetallic bulk bismuth, ultrathin Bi(111) films are expected to be topological insulators. Our study may therefore pave the way for the generation of high quality Bi nanostructures to be used in spin electronics.

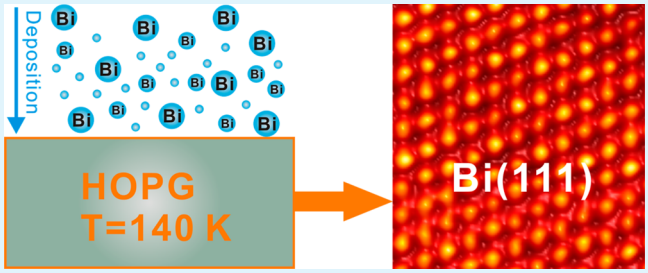

KEYWORDS: *bismuth nanostructures, highly oriented pyrolytic graphite scanning, tunneling microscopy, photoemission spectroscopy*

INTRODUCTION

Bismuth is a promising semimetal and exhibits a rich variety of physical properties such as high resistivity and Hall coefficient and large thermoelectric power,[1−3] mostly attributed to its small electron/hole effective masses and lower carrier density.[4−7] In particular, owing to the tiny electron/hole pockets at the L and T points of the bulk Brillouin Zone, bismuth has an extremely long Fermi wavelength (in the order of tens of nanometers), which is comparable to the thickness of thin films; therefore, quantum size effect (QSE) may easily emerge in thin film systems due to the confinement of electron in the direction perpendicular to the surface.[6−9] More interestingly, bilayer Bi(111) has been recently predicted to be a topological insulator and shows novel electronic properties,[10] which further enhances the interest in bismuth thin films. All these features suggest bismuth as an ideal candidate for the study of quantum size effects with potential for exploitation in prospective nanoelectronics.[6−8] In addition, properties of different nanostructures (i.e., thin films, nanowires (NWs), and nanoparticles/islands) differ significantly from each other and also from their bulk materials due to the dimensionality limit.[11,12] Therefore, fabrication of diverse bismuth nanostructures on nonmetallic substrates has attracted significant attention during the past years; for example, the growth of thin bismuth films has been studied on different surfaces, such as on Si(111),[7,13−16] Si(001),[17] SiO_2,[18] glass,[19] InAs,[20] graphene,[21,22] and Bi_2Te_3.[23,24] Within these studies, the growth mode of Bi nanostructures and quantum size effects such as quantum well states (QWS) and topological insulator states (TIS) have been well addressed and exploited.[15,16,21−25]

Highly oriented pyrolytic graphite (HOPG) has also been widely used as a substrate for investigating the growth process of nanostructures.[26−28] The inertness of the graphite surface as well as its atomic smoothness makes it an ideal template for the growth of free-standing clusters and nanostructures. Moreover, the well-known cleaving process of HOPG can easily introduce decorating step edges to the substrate, which offers controllable defect traps for the guided growth or formation of nanostructures. The growth process of large scale bismuth networks on HOPG has been investigated intensively mainly by Brown and co-workers.[29−34] By varying the growth conditions, they studied in detail the possible mechanism of forming Bi(110) crystal surfaces below the critical thickness.[31,32] As reported by Nagao et al.,[15] bismuth usually prefers the black-phosphorus structure instead of the rhombohedral structure at a small thickness (below 6 monolayers). Bi(111) is the favored plane for thicker films because of the higher cohesive energy relative to (110), but for the small thicknesses, this situation is

Received: January 10, 2015
Accepted: April 7, 2015
Published: April 7, 2015

DOI: 10.1021/acsami.5b00264
ACS Appl. Mater. Interfaces 2015, 7, 8525−8532

inverted. In spite of this, ultrathin Bi(111) films on Bi_2Te_3 have been successfully realized recently in experiments,[23,24] and TIS from Bi(111) thin film were observed as predicted. All these exciting observations highlight the remaining challenge of growing ultrathin Bi(111)film on HOPG. Since the HOPG substrate and the Bi(111) crystal surface both have a layered hexagonal lattice, it is believed that, by tuning the kinetics of the film growth (for example, by low-temperature deposition or by surfactant mediated growth), ultrathin Bi(111) layers on top of HOPG should be accessible at an atomic thickness.[23]

Having understood the special properties of bulk Bi, it is even more appealing to manipulate its electronic structure through ultrathin films on inert substrates and to switch Bi from a semimetal (bulk) to an insulator,[6−8,23,24] which can be crucial in tuning physical properties (such as electrical conductance, transport properties, etc.) of related devices and electronics. Moreover, with the possibility of building (111)-faceted thin films on an inert HOPG substrate, one can produce Bi(111)-like surface properties without the need for a bulk Bi substrate. Since the Bi(111) thin films behave as topological insulators, Bi(111) faceted nanostructures may facilitate potential application in spintronic devices. In this regard, we report the experimental observation of Bi(111) nanofilms grown on HOPG at low temperature (140 K), which demonstrates the feasibility of constructing (111) oriented islands on top of HOPG and bridges the gap among previous reports.[13−16,29−33] With a combination of scanning tunneling microscopy (STM), ultraviolet photoelectron spectroscopy (UPS), X-ray photoelectron spectroscopy (XPS), and low energy electron diffraction (LEED), the structural and electronic state of the Bi islands on HOPG are reported and discussed. In this respect, this study is of high importance since it shows how 2D material can be tuned from (110) oriented growth to (111) facet by changing the growth temperature, allowing for the possible study of a single constituent topological material which is crucially important for fabricating topologically based spin polarized systems to be used in spintronic devices.

EXPERIMENTAL DETAILS

All the experiments were carried out in an ultrahigh vacuum (UHV) system with base pressure better than 10^{-10} mbar, equipped with a variable temperature STM (Omicron) and a hemispherical analyzer (PHOIBOS 150, SPECS, the instrumental energy resolution was 50 meV). Commercially available HOPG (Goodfellow) was transferred into the UHV chamber immediately after cleaving in air. Prior to deposition, the HOPG substrates were degassed at 700 K for several hours in order to remove the adsorbed contamination. Flat terraces with several hundred nanometers separated by steps are easily achieved by cleaving concluded from STM measurements. High purity bismuth (99.999%) was thermally evaporated in UHV from a homemade Tantalum pocket, while the HOPG substrate was kept at 140 K during the deposition. UPS was measured using the Helium I line (21.2 eV) of a high-intensity gas discharge lamp in the lab and calibrated with the Ta Fermi edge. XPS was recorded with Al Kα radiation with a photon energy of 1468.6 eV and calibrated by the Ta 4f core level. STM images were taken at 90K in a constant-current mode, using electrochemically etched W tips. The STM images were acquired using a current set point of 0.3 nA and a bias voltage of 1.2 V. The image scales were calibrated with the periodic structures and atomic steps on HOPG. Image processing was done using the free software WSxM.[35] Bismuth is characterized with rhombohedra symmetry in an A7 structure, which is typical for the group V semimetals (space group *R*3*m*, arsenic structure).[8] There are three different indexing systems to describe the Bi bulk structure: rhombohedral, hexagonal, and pseudocubic; herein, we adopt the rhombohedra indices.

RESULTS AND DISCUSSION

The morphology evolution of bismuth nanostructures with increasing coverage are presented by a series of STM images in Figure 1. The deposition flux was fixed at around 0.1 Å/min

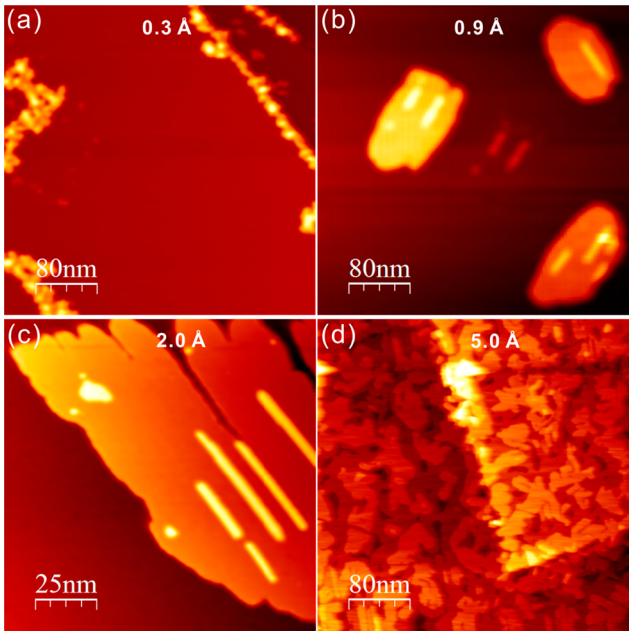

Figure 1. Typical STM images showing the morphology evolution of Bi nanostructures on HOPG prepared at 140 K. Coverage: (a) 0.3 Å, (b) 0.9 Å, (c) 2.0 Å, and (d) 5.0 Å. Tunneling parameters: V = 1.2 V, I = 0.3 nA.

while the HOPG substrate was kept at 140 K. Figure 1a shows the topography of the bismuth film at a deposited thickness of 0.3 Å, whereas decorating Bi clusters first start to assemble. The Bi nucleation appears to be somewhat disordered due to the fact that nucleation occurs at step edges. Additional nucleation of bismuth atoms on flat terraces between step edges also occurs at higher coverage. A similar behavior has been reported before[29,30] when thin Bi film was prepared on HOPG kept at room temperature, which indicates the high mobility of Bi atoms on the flat terraces regardless of the substrate temperature. Increasing the coverage to 0.9 Å leads to the formation small islands on flat terraces. Besides the formation of these well-orientated islands, one-dimensional (1D) nanowires (NWs) emerge as well. Upon further deposition (2.0 Å), larger areas of "finger-shaped" 2D islands were formed, as seen from the magnified STM image of the surface in Figure 1c. These 2D islands are distributed over the terraces, and it appears that additional Bi atoms arrange as NWs on top of these 2D islands even before completion of the first "layer". An estimation of the relative areas indicates that the percentage of 1D NWs is quite small (5%) compared to 2D islands. This observation indicates a high edge-diffusion barrier (Schweobel barrier), which as a result makes the diffusion of Bi atoms over the HOPG surface into a complete "layer" less feasible.[36] Further deposition (5 Å bismuth in total) results in a similar architecture and indicates that the additional Bi layers are sitting on top of the incomplete bismuth films, as shown in Figure 1d, which again suggests the higher edge-diffusion

DOI: 10.1021/acsami.5b00264
ACS Appl. Mater. Interfaces 2015, 7, 8525−8532

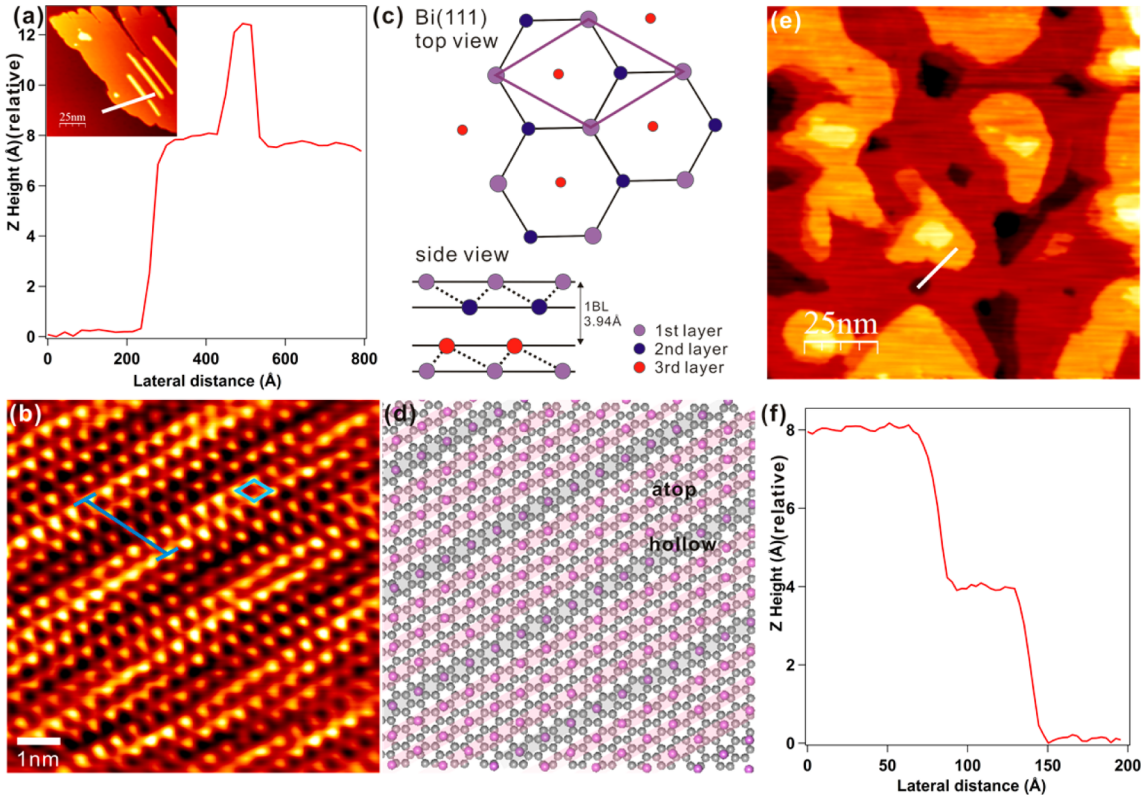

Figure 2. Close-up investigations of the 2D islands at a coverage of 2.0 Å. (a) STM height profile along the direction indicated by the white line in the inset. The 2D islands are a height of 8 Å above the HOPG substrate, while the NWs on top of the 2D islands have an addition height of 4 Å. (b) A zoom-in STM investigation on the 2D island from Figure 1c (as shown in the inset of (a)), where the hexagonal structure is concluded and the rhombic unit cell is highlighted by the blue rhombus. (c) Crystal structure of Bi(111) surface. The top and side views are shown explicitly with the unit cell. (d) Simulated Moiré pattern of the Bi(111) layer on top of the graphite layer using the simple superposition method. Gray: Carbon atom; purple: bismuth atom. (e) and (f) STM line profile drawn on the thick film, following the direction indicated by the white line in (e). Tunneling current: 0.2 nA; bias voltage: 1.0 V.

barrier for Bi adatoms on HOPG and prevents the development of a complete film. The growth mode herein slightly differs from the conventional layer-by-layer behavior, where complete films form prior to the growth of subsequent layers.[37] This defective layer-by-layer growth process shows that bismuth atoms are rather mobile on the HOPG terraces, and the interaction between bismuth adatoms/adlayers is much stronger than the interaction between bismuth film and the substrate, which was evidenced by the core level measurements of Bi 4f and C 1s, as discussed in the XPS section.

In order to determine the preferred crystallographic orientation of bismuth films on HOPG, a detailed investigation of these 2D islands at the coverage of 2.0 Å was carefully performed. First, typical heights of islands and nanowires (as from Figure 1c) are presented by the line profile in Figure 2a, following the direction as indicated by the white line in the inset in Figure2a. Heights of 8 and 4 Å with an uncertainty of 0.15 Å were commonly observed for 2D islands and nanowires/nanostructures on top (these values were averaged from line profiles from about a hundred images rendering the uncertainty, and a height of 8 Å was also found for the islands at the Bi coverage of 0.9 Å), similar to that of a moderate coverage of bismuth on HOPG reported by Brown and co-workers.[29] One bilayer (BL) Bi(111) has a thickness of 3.94 Å (the structure model is shown in Figure 2c); therefore, 4 Å (8 Å) should be related to 1 (2) BL of Bi(111) film, as clarified in the case of Bi on Bi_2Se_3 reported by Jia and co-workers.[24] Atomically resolved images reveal that remarkably smooth and flat bismuth layers were formed at this coverage, as seen in Figure 2b. Furthermore, the hexagonal structure is clarified from analysis with the rhombic unit cell indicated by the blue rhombus in Figure 2b, and the lattice distance is found to be around 4.3 Å (as verified by LEED measurements, which will be discussed later). Moiré effect was easily recognized from the pattern in Figure 2b with an apparent periodicity of approximate 4 unit cells of the Bi layers in the labeled direction, which is probably due to the lattice mismatch between the HOPG and Bi layers, and a similar behavior of Bi thin film on HOPG was also reported by Brown and co-workers.[38] Moiré pattern is directed almost in the same direction as the unit cell vector and has an approximate periodicity of 4 times the Bi(111) lattice distance ($4 \times 4.3 = 1.720$ nm), which is almost commensurate with the underlying HOPG with 7 units of cell distance ($7 \times 2.456 = 1.719$ nm). Moreover, the Bi(111) layer is misorientated around 2° with respect to the HOPG substrate. When bismuth atoms are arranged on top or nearly atop of carbon atoms, bright dots are observed from STM image, while a relatively dark pattern is formed if Bi atoms are sitting on the hollow site or near the hollow site of HOPG. Using the simple superposition method introduced from Brown and co-workers,[38] the Bi(111) layer was laid on top of a graphite layer substrate and the simulated Moiré pattern was presented in Figure 2d for comparison. Good agreement between the experimental image and the simulation was concluded. However, we notice that this Moiré

DOI: 10.1021/acsami.5b00264
ACS Appl. Mater. Interfaces 2015, 7, 8525−8532

pattern is only one-dimensional, which is probably due to the symmetry breaking induced by the lattice strain.

A similar hexagonal structure was also proposed by Wang and co-workers[39] for antimony (Sb, another group V element) on HOPG. Moreover, these STM observations point out that a buffer bilayer was initially introduced directly on contacting the HOPG substrate prior to the construction of successive 2D ordered islands (8 Å − 4 Å = 4 Å). Similarly, a wetting layer or intermediate layer is also reported by other studies;[14,15,32,40] the possible mechanism here for forming the buffer bilayer could be related to the lattice strain relaxation.[41,42] Since the unit cell parameter of the surface structure indicates a $(\sqrt{3} \times \sqrt{3})$ R30° reconstruction with respect to the HOPG substrate ($\sqrt{3} \times$ HOPG lattice distance 2.46 Å = 4.3 Å) and the intrinsic Bi(111) crystal structure has a lattice distance of 4.54 Å, a buffer layer is necessary for the relaxation of strain due to the slight lattice mismatch (from the bulk value of 4.54 Å to the reconstructed surface structure of 4.30 Å, compressed by 5%). However, detailed information about this buffer bilayer is unfortunately unknown, except the height profile and the Moiré effect.[33,38] The bulk crystal structure of the Bi(111) surface with top and side views are also illustrated in Figure 2c for direct comparison. Notably, the morphology of bismuth nanostructures on HOPG is different from the observation of Bi(111) films on Bi_2Te_3[24] and is consistent with the behavior of Bi(111) bilayers on the Bi(111) substrate,[43] which are probably due to the different boundary conditions from the varying substrates. Another indication of the formation of a Bi(111) bilayer is the STM height profile of a 5 Å thick Bi film (as seen in Figure 2e with higher magnification in Figure 1d), which shows again a step height of 4.0 Å with respect to the film underneath (as seen in Figure 2f; Note that here the height profile is relative; as can be seen from dark holes, there are Bi layers underneath the topmost 4 Å Bi bilayer). Therefore, it seems that the Bi(111) phase is also preserved for thick coverage, consistent with the well-known fact that Bi(111) is the preferred direction for epitaxial growth on many solid substrates.[8,15] Moreover, it can be concluded that the growth of Bi starts from 2 BL with the first BL as buffer layer in a defect nucleated manner and continues with an increase of integer bilayer subsequently on HOPG at low temperature.

As discussed in the Introduction, bismuth usually grows with a (110) phase at ultrathin coverage below the critical thickness and transforms into the bulk-like crystal (111) phase above the critical thickness. However, as reported by Nagao et al.,[15] this critical thickness varies depending on external condition in practice proportionally to the substrate temperature during deposition. Therefore, the critical thickness will be smaller when Bi is deposited onto a colder substrate. Therefore, by choosing the proper substrate with a similar hexagonal structure and, most crucially, with moderate interaction to the islands, it is possible in the end to grow a Bi(111) phase on top of HOPG at low temperature. It is worth pointing out that there is a defect or edge step nucleated growth of Bi on HOPG in our study, which induces the formation of elongated islands, and substrate directional growth for the larger islands is rarely found at thinner Bi coverage, as is clearly seen in Figure 1a−c. Actually, similar behaviors have also been reported in earlier studies. For example, an Na layer was grown on graphite with close packed structure (rhombic unit cell),[44] and elongated shapes of islands were regularly observed due to the rate limiting conditions of deposition and diffusion with respect to adsorption sites, nucleation sites, and diffusivity. Elongated domains of striped Fe(111) structure were also reported by Yokogawa and co-workers.[45] These observations suggest that dislocation boundaries can be formed across the whole island that may serve as nucleation sites for adatoms on top of the islands.

LEED measurements were also carried out to verify the conclusion of the crystallographic orientation of bismuth film on HOPG drawn from STM measurements. Figure 3a is the

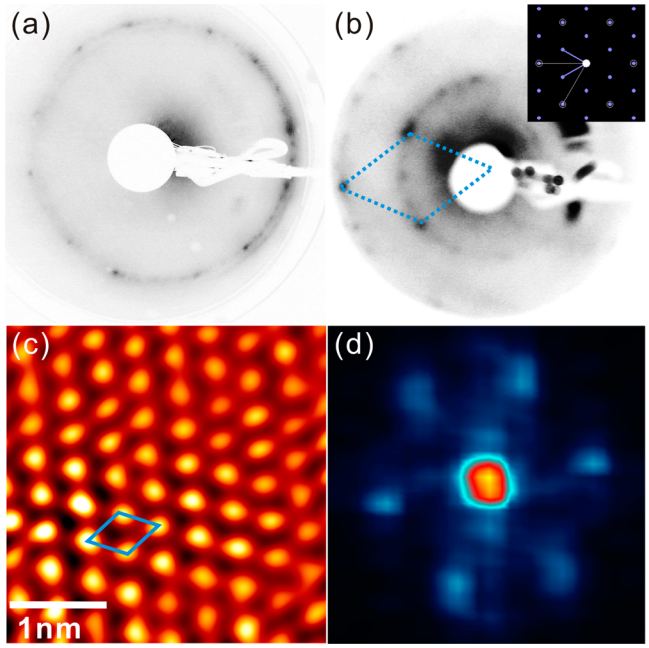

Figure 3. (a) LEED pattern of HOPG and (b) 2 Å Bi on top of HOPG taken at beam energy of 66 eV at 140 K. Two rotated domains with 1 × 1 pattern are dominating in the clean HOPG, which indicates the high quality of the cleaved surface, while a 2.0 Å thick Bi film forms a $\sqrt{3} \times \sqrt{3}$ hexagonal structure on top of HOPG. (c) An atomically resolved STM image reveals the hexagonal structure of the Bi film. (d) The fast Fourier transform (FFT) of (c), which is consistent with the LEED pattern from (b).

LEED pattern of the clean HOPG substrate at a beam energy of 66 eV, where two domains with different azimuthal orientation could easily be recognized (12 spots comprise the first order pattern). Usually, a ring pattern is observed for HOPG due to the existence of a large number of micron-size crystallites owing different crystal orientations. In our study, by carefully handling the substrate, we managed to reproduce high-quality graphite surfaces mainly containing two rotated domains with a sharp 1 × 1 pattern in the detectable area (several micrometers).[46] When 2 Å bismuth is deposited onto HOPG kept at 140 K, as presented in Figure 3b, a smaller ring is formed inside the pristine outer ring, which is definitely due to the Bi adsorption. As is judged from the radius of these two rings, the ratio of the inner ring to the outer ring is 0.59:1, which corresponds to a $(\sqrt{3} \times \sqrt{3})$ reconstruction of the Bi layer on top of HOPG. Notably, more spots are seen in the outer ring in Figure 3b compared to Figure 3a, which is due to the mixed contribution of misorientated and multiple domain bismuth layers. In order to make it easy to explain, a simulated LEED pattern for the single domain Bi $(\sqrt{3} \times \sqrt{3})$ structure on HOPG is represented in the inset of Figure 3b. As is seen from the simulated pattern, the original HOPG spots overlap a part of the second order LEED pattern of the Bi layer, which means

DOI: 10.1021/acsami.5b00264
ACS Appl. Mater. Interfaces 2015, 7, 8525−8532

misorientated or multiple domain Bi(111) structures will also have the same ring-like pattern as HOPG. The presence of the inner ring-like pattern is due to the same mechanism as that for the outer ring: the coexistence of misorientated and multiple domain Bi(111) layer and therefore the mixture of differently orientated hexagonal pattern (the first order LEED pattern from the Bi(111) structure) comprises the inner ring.

From the LEED analysis, it is now possible to draw the conclusion that the Bi(111) layer on top of HOPG has a lattice distance of around 4.3 Å. This LEED observation manifests the formation of Bi(111) crystal surface on HOPG. On the other hand, the Bi(110) facet would instead show a rather complex pattern as predicted.[38,47,48] This is further supported by the fast Fourier transformation analysis of the atomically resolved STM image, which indicates a clear hexagonal lattice and is consistent with the LEED data (Figure 3c,d).

When two different semimetals are combined together, behaviors such as the formation of quantum wells, band alignment, or charge transfer on the interface should be observable at varying film thickness,[49] as already reported for Bi(110) on HOPG by Brown and co-workers.[50] Consequently, valence band (VB) spectroscopy was performed to detect whether such phenomena exists or not. Figure 4 shows the evolution of valence band as a function of bismuth coverage at 140 K. The uppermost spectrum in Figure 4a was recorded on a thick film (33.0 Å). It essentially represents bismuth bulk-like features with the sharp surface state at about 0.2 eV below the Fermi level.[8] The other spectra were obtained in sequence on films with thicknesses of 0.75, 1.5, 2.7, 4.9, 11.1, and 33.0 Å, respectively. As indicated in Figure 4, respective peaks originating from different bismuth bands[8] are identified with dashed lines, and changes of the corresponding peaks are marked as well. From the evolution of the VB, one can recognize that peaks evolve from quantum well confined states for thin islands to fully developed bulk-like features. At the thick coverage of 33 Å, bulk-like features including the surface state (SS) at 0.2 eV and the sp bands at 1.1 and 2.6 eV, respectively, below the Fermi level are predominant, and all the other peaks become less visible.

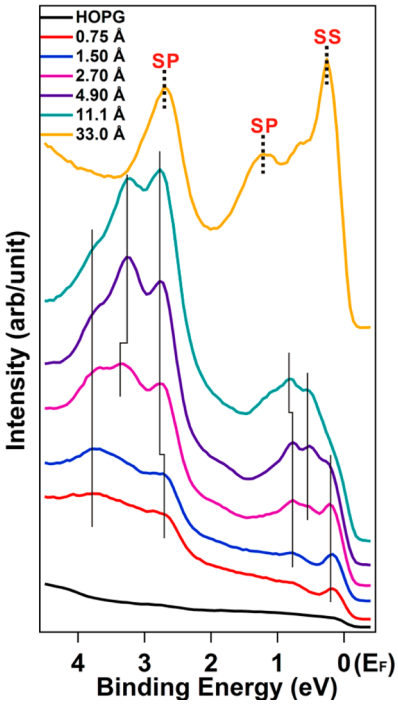

Figure 4. . Valence band evolution of the Bi nanostructures on HOPG as a function of film thickness. The spectra were recorded at 140 K, and shifts of peaks coming from different bismuth bands are labeled with continued dashed lines.

The behavior in UPS spectra is consistent with the initial formation and evolution of quantum well states as revealed by the DFT calculation of the density of states (DOS) for varying Bi bilayers on HOPG[50] and the experimental observation of Bi thin film on Si(111).[16] Although the acquired data set is not extensive enough to properly assign the quantum numbers to these bands, they are no longer observable at a sufficient film thickness of 33 Å, where the observed bands are originating from more bulk-like features: the bulk sp bands at 1.1 and 2.6 eV, respectively, and the SS at 0.2 eV are the dominant spectral features. As reported by Brown et al.,[50] charge transfer can also happen at such a Bi/HOPG interface which may contribute to the shift of observed peaks, but it is difficult to draw a conclusion here with the available UPS spectra whether a charge transfer happens across the interface, while the dominant contribution to the shift of peaks should be from the evolution of quantum well states to bulk-like features. In all, the evolution of VB here agrees well with that of the typical hybrid heterojunction system where different films with unequal band gaps are engineered in layered structures.[49,50]

To gain deeper insight into the growth mechanism and the interaction between bismuth nanostructures and HOPG, XPS of Bi 5f and C 1s core levels was measured to determine the adhesive interaction between bismuth adatoms and the HOPG substrate at different film thicknesses. As seen from Figure 5a, a pair of peaks with energy difference of 5.8 eV (Bi $4f_{5/2}$, 162.4 eV; Bi $4f_{7/2}$, 156.6 eV) due to the spin−orbital splitting was recognized immediately from Bi 4f core level spectra.[51] The C 1s consisting of only one component was located at 284.6 eV (Figure 5b), which was the typical position for C 1s originating from graphite.[52] As expected, no shift for Bi 4f or C 1s was found during the growth process from ultrathin film to rather thick film. The stable binding energy of Bi 4f and C 1s implies that no chemical bonding was formed between Bi atoms and HOPG atoms at the interface and the formation of Bi films is mostly dominated by the adhesive attraction between Bi adatoms, which firmly supports the conclusion drawn from STM measurements that the adsorbate−substrate interaction is rather weak compared to the interaction between bismuth adatoms/adlayers and is consistent with other reports of Bi on HOPG at room temperature by Brown and co-workers.[32,33] Moreover, changes of the peak intensity of Bi 4f and C 1s in Figure 5 were analyzed after proper curve fitting, showing a nearly exponential increase for Bi 4f and an exponential attenuation for C 1s, which also supports the quasi layer-by-layer growth mode of bismuth nanostructures on HOPG except at low coverage. As already seen from STM images (Figure 1c), the growth of strips on top of the Bi islands is already found at low coverage. For all the other coverages, an island height distribution displaying 2 to 3 different bilayers was found, which is consistent with a layer-by-layer growth.

Finally, it is also worth reiterating that it is appealing to be able to manipulate bismuth's special bulk properties to facilitate an electronic transition from semimetal to topological insulator or semiconductor, by suitable control over the thin film growth parameters This can be crucial in tuning the physical properties

DOI: 10.1021/acsami.5b00264
ACS Appl. Mater. Interfaces 2015, 7, 8525−8532

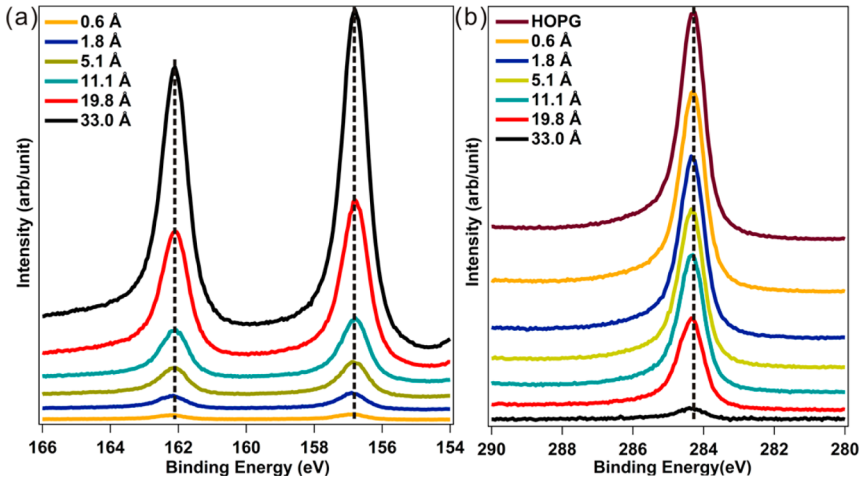

Figure 5. XPS records of Bi 4f (a) and C 1s (b) during the growth of Bi film from ultrathin coverage to thick film. No shift of Bi 4f or C 1s was observed during the growth process, indicating the rather weak bonding between the Bi adsorption and HOPG substrate.

(such as electrical conductance, transport property, and so on) of related thin film devices and nanoelectronics. Moreover, with the possibility of building (111)-faceted thin films on an inert HOPG substrate, we can produce Bi(111)-like surface properties without having the bulk Bi material. Since Bi(111) thin films behave as topological insulators, our report may facilitate potential applications in spintronic devices. In this respect, this study is of high importance since it offers an approach to directly fabricate Bi(111) thin films and it also shows how 2D materials can be tuned from (110) oriented growth to (111) facets by changing the growth temperature, allowing for the possible study of a single constituent topological material. All these factors are important for fabricating topological insulator based systems with spin polarized properties and may facilitate bismuth's potential application used in spintronic devices.

CONCLUSION

In conclusion, we have demonstrated that the formation of (111) oriented bismuth islands on HOPG is the preferred growth mode when the substrate is kept at 140 K during deposition. The growth process was investigated thoroughly by a combination of STM, UPS, XPS, and LEED. As expected, the Bi(111) surface as the preferred facet grew in the form of bilayers when deposited onto the as-cleaved cold HOPG substrate, and the Bi(111) crystallinity orientation was preserved from low coverage to thick films. XPS investigation of both C 1s and Bi 4f core level reflects the rather weak bonding between the Bi film and the HOPG substrate and supports the quasi layer-by-layer like growth mode of Bi nanostructures on HOPG at low temperature. Moreover, the evolution of the valence band at the interface is recorded by UPS and the transition from quantum well states to bulk-like features is discovered for increasing film thickness. As is well-known, the epitaxial growth of high-quality two-dimensional bismuth films is a promising approach toward the application of spintronics devices, especially the topological-insulator Bi(111) ultrathin film. Our study here may indicate a route to grow high quality Bi(111) thin film on HOPG and provide a basis for the exploration of possible usage in spin electronics.

AUTHOR INFORMATION

Corresponding Authors

*E-mail: songfei@sinap.ac.cn.

*E-mail: erik.wahlstrom@ntnu.no.

Author Contributions

The manuscript was written through contributions of all authors. All authors have given approval to the final version of the manuscript.

Funding

This work was financially supported by the Norwegian Research Council (project 171332/V30 under the FriNat program and project 182037/S10 under the NANOMAT program) and the Hundred Talents project of the Chinese Academy of Sciences.

Notes

The authors declare no competing financial interest.

ACKNOWLEDGMENTS

Fruitful discussions with Dr. Balasubramanian Thiagarajan, Dr. Zheshen Li, and Prof. Anne Borg were greatly acknowledged.

REFERENCES

(1) Yang, F. Y.; Liu, K.; Hong, K.; Reich, D. H.; Searson, P. C.; Chien, C. L. Large Magnetoresistance of Electrodeposited Single-Crystal Bismuth Thin Films. *Science* **1999**, *284*, 1335.

(2) Weitzel, B.; Micklitz, H. Superconductivity in Granular Systems Built from Well-Defined Rhombohedral Bi-Clusters: Evidence for Bi-Surface Superconductivity. *Phys. Rev. Lett.* **1991**, *66*, 385.

(3) Hoffman, C. A.; Meyer, J. R.; Bartoli, F. J.; Di Venere, A.; Yi, X. J.; Hou, C. L.; Wang, H. C.; Ketterson, J. B.; Wong, G. K. Semimetal-to-Semiconductor Transition in Bismuth Thin Films. *Phys. Rev. B* **1993**, *48*, 11431.

(4) Ast, C.; Höchst, H. Fermi Surface of Bi(111) Measured by Photoemission Spectroscopy. *Phys. Rev. Lett.* **2001**, *87*, 177602.

(5) Ogrin, Y. F.; Lutskii, V. N.; Elinson, M. I. Observation of Quantum Size Effects in Thin Bismuth Films. *JETP Lett.* **1966**, *3*, 71–73.

(6) Zhang, Z.; Sun, X.; Dresselhaus, M.; Ying, J.; Heremans, J. Electronic Transport Properties of Single-Crystal Bismuth Nanowire Arrays. *Phys. Rev. B* **2000**, *61*, 4850.

(7) Hirahara, T.; Nagao, T.; Matsuda, I.; Bihlmayer, G.; Chulkov, E. V.; Koroteev, Y. M.; Hasegawa, S. Quantum Well States in Ultrathin Bi Films: Angle-Resolved Photoemission Spectroscopy and First-Principles Calculations Study. *Phys. Rev. B* **2007**, *75*, 035422.

DOI: 10.1021/acsami.5b00264
ACS Appl. Mater. Interfaces 2015, 7, 8525–8532

(8) Hofmann, P. The Surfaces of Bismuth: Structural and Electronic Properties. *Prog. Surf. Sci.* **2006**, *81*, 191−245.
(9) Dil, J. H.; Kampen, T. U.; Hülsen, B.; Seyller, T.; Horn, K. Quantum Size Effects in Quasi-Free-Standing Pb Layers. *Phys. Rev. B* **2007**, *75*, 161401(R).
(10) Liu, Z.; Liu, C. X.; Wu, Y. S.; Duan, W. H.; Liu, F.; Wu, J. Stable Nontrivial Z2 Topology in Ultrathin Bi (111) Films: A First-Principles Study. *Phys. Rev. Lett.* **2011**, *107*, 136805.
(11) Alivisatos, A. P. Semiconductor Clusters, Nanocrystals, and Quantum Dots. *Science.* **1996**, *271*, 933.
(12) Moriarty, P. Nanostructured Materials. *Rep. Prog. Phys.* **2001**, *64*, 297.
(13) Yaginuma, S.; Nagao, T.; Sadowski, J. T.; Pucci, A.; Fujikawa, Y.; Sakurai, T. Surface Pre-Melting and Surface Flattening of Bi Nanofilms on Si(1 1 1)-7*7. *Surf. Sci.* **2003**, *547*, L877−L881.
(14) Nagao, T.; Yaginuma, S.; Saito, M.; Kogure, T.; Sadowski, J. T.; Ohno, T.; Hasegawa, S.; Sakurai, T. Strong Lateral Growth and Crystallization via Two-Dimensional Allotropic Transformation of Semi-Metal Bi Film. *Surf. Sci.* **2005**, *590*, L247−L252.
(15) Nagao, T.; Sadowski, J. T.; Saito, M.; Yaginuma, S.; Fujikawa, Y.; Kogure, T.; Ohno, T.; Hasegawa, Y.; Hasegawa, S.; Sakurai, T. Nanofilm Allotrope and Phase Transformation of Ultrathin Bi Film on Si(111)-7*7. *Phys. Rev. Lett.* **2004**, *93*, 105501.
(16) Hirahara, T.; Nagao, T.; Matsuda, I.; Bihlmayer, G.; Chulkov, E. V.; Koroteev, Yu. M.; Echenique, P. M.; Saito, M.; Hasegawa, S. Role of Spin-Orbit Coupling and Hybridization Effects in the Electronic Structure of Ultrathin Bi Films. *Phys. Rev. Lett.* **2006**, *97*, 146803.
(17) Owen, J. H. G.; Miki, K.; Koh, H.; Yeom, H. W.; Bowler, D. R. Stress Relief as the Driving Force for Self-Assembled Bi Nanolines. *Phys. Rev. Lett.* **2002**, *88*, 226104.
(18) Kusz, B.; Pliszka, D.; Gazda, M.; Brusa, R. S.; Trzebiatowski, K.; Karwasz, G. P.; Zecca, A.; Murawski, L. Structural Studies of Bismuth Nanocrystals Embedded in SiO_2 or GeO_2 Matrices. *J. Appl. Phys.* **2003**, *94*, 7270−7275.
(19) El-Sayed, N. Z. Physical Characteristics of Thermally Evaporated Bismuth Thin Films. *Vacuum* **2006**, *80*, 860−863.
(20) Ahola-Tuomi, M.; Laukkanen, P.; Punkkinen, M. P. J.; Perälä, R. E.; Väyrynen, I. J.; Kuzmin, M.; Schulte, K.; Pessa, M. Formation of an Ordered Pattern of Bi Nanolines on InAs(100) by Self-Assembly. *Appl. Phys. Lett.* **2008**, *92*, 011926.
(21) Sun, J. T.; Huang, H.; Wong, S. L.; Feng, Y. P.; Wee, A. T. S. Energy-Gap Opening in a Bi(110) Nanoribbon Induced by Edge Reconstruction. *Phys. Rev. Lett.* **2012**, *109*, 246804.
(22) Huang, H.; Wong, S. L.; Wang, Y. Z.; Sun, J. T.; Gao, X. Y.; Wee, A. T.S. Scanning Tunneling Microscope and Photoemission Spectroscopy Investigations of Bismuth on Epitaxial Graphene on SiC(0001). *J. Phys. Chem. C* **2014**, *118*, 24995−24999.
(23) Hirahara, T.; Bihlmayer, G.; Sakamoto, Y.; Yamada, M.; Miyazaki, H.; Kimura, S. I.; Blügel, S.; Hasegawa, S. Interfacing 2D and 3D Topological Insulators: Bi(111) Bilayer on Bi_2Te_3. *Phys. Rev. Lett.* **2011**, *107*, 166801.
(24) Yang, F.; Miao, L.; Wang, Z. F.; Yao, M. Y.; Zhu, F. F.; Song, Y. R.; Wang, X. M.; Xu, J. P.; Fedorov, A. V.; Sun, Z.; Zhang, G. B.; Liu, C. H.; Liu, F.; Qian, D.; Gao, C. L.; Jia, J. F. Spatial and Energy Distribution of Topological Edge States in Single Bi(111) Bilayer. *Phys. Rev. Lett.* **2012**, *109*, 016801.
(25) Gao, C. L.; Qian, D.; Liu, C. H.; Jia, J. F.; Liu, F. Topological Edge States and Electronic Structures of a 2D Topological Insulator: Single-Bilayer Bi (111). *Chin. Phys. B* **2013**, *22*, 067304.
(26) Henry, C. R. Surface Studies of Supported Model Catalysts. *Surf. Sci. Rep.* **1998**, *31*, 231.
(27) Binns, C.; Baker, S. H.; Demangeat, C.; Parlebas, J. C. Growth, Electronic, Magnetic and Spectroscopic Properties of Transition Metals on Graphite. *Surf. Sci. Rep.* **1999**, *34*, 105.
(28) Jensen, P. Growth of Nanostructures by Cluster Deposition: Experiments and Simple Models. *Rev. Mod. Phys.* **1999**, *71*, 1695.
(29) Scott, S. A.; Kral, M. V.; Brown, S. A. A Crystallographic Orientation Transition and Early Stage Growth Characteristics of Thin Bi Films on HOPG. *Surf. Sci.* **2005**, *587*, 175−184.
(30) Scott, S. A.; Milo, V. K.; Brown, S. A. Growth of Oriented Bi Nanorods at Graphite Step-Edges. *Phys. Rev. B* **2005**, *72*, 205423.
(31) McCarthy, D. A.; Robertson, D.; Kowalczyk, P. J.; Brown, S. A. The Effects of Annealing and Growth Temperature on The Morphologies of Bi Nanostructures on HOPG. *Surf. Sci.* **2010**, *604*, 1273−1282.
(32) Kowalczyk, P. J.; Mahapatra, O.; McCarthy, D. N.; Kozlowski, W.; Klusek, Z.; Brown, S. A. STM and XPS Investigations of Bismuth Islands on HOPG. *Surf. Sci.* **2011**, *605*, 659−667.
(33) Kowalczyk, P. J.; Mahapatra, O.; Brown, S. A.; Bian, G.; Wang, X.; Chiang, T.-C. Electronic Size Effects in Three-Dimensional Nanostructures. *Nano Lett.* **2013**, *13*, 43−47.
(34) Kowalczyk, P. J.; Mahapatra, O.; Brown, S. A.; Bian, G.; Chiang, T.-C. STM Driven Modification of Bismuth Nanostructures. *Surf. Sci.* **2014**, *621*, 140−145.
(35) Horcas, I.; Fernandez, R.; Gomez-Rodriguez, J. M.; Colchero, J.; Gomez-Herrero, J.; Baro, A. M. WSXM: A Software for Scanning Probe Microscopy and a Tool for Nanotechnology. *Rev. Sci. Instrum.* **2007**, *78*, 013705.
(36) Brune, H. Microscopic View of Epitaxial Metal Growth: Nucleation and Aggregation. *Surf. Sci. Rep.* **1998**, *31*, 122−229.
(37) Venables, J. A. *Introduction to Surface and Thin Film Processes*; Cambridge University Press: Cambridge, 2000.
(38) Kowalczyk, P. J.; Mahapatra, O.; Belić, D.; Brown, S. A.; Bian, G.; Chiang, T.-C. Origin of the Moiré Pattern in Thin Bi Films Deposited on HOPG. *Phys. Rev. B* **2015**, *91*, 045434.
(39) Yan, Z.; Kushvaha, S. S.; Xiao, W.; Wang, X. S. Different-Dimensional Structures of Antimony Formed Selectively on Graphite. *Appl. Phys. A: Mater. Sci. Process.* **2007**, *88*, 299−307.
(40) Sharma, H. R.; Fournée, V.; Shimoda, M.; Ross, A. R.; Lograsso, T. A.; Gille, P.; Tsai, A. P. Growth of Bi Thin Films on Quasicrystal Surfaces. *Phys. Rev. B* **2008**, *78*, 155416.
(41) Schumann, T.; Dubslaff, M.; Oliveira, M. H.; Hanke, M., Jr.; Lopes, J. M. J.; Riechert, H. Effect of Buffer Layer Coupling on the Lattice Parameter of Epitaxial Graphene on SiC(0001). *Phys. Rev. B* **2014**, *90*, 041403(R).
(42) Suda, J.; Miura, K.; Honaga, M.; Nishi, Y.; Onojima, N.; Matsunami, H. Relaxation of AlN Buffer Layers in Molecular-Beam Epitaxial Growth of GaN. *Appl. Phys. Lett.* **2002**, *81*, 5141.
(43) Jnawali, G.; Wagner, T.; Hattab, H.; Moller, R.; Horn-von Hoegen, M. Nucleation and Initial Growth in the Semimetallic Homoepitaxial System of Bi on Bi(111). *Phys. Rev. B* **2009**, *79*, 193306.
(44) Breitholtz, M.; Kihlgren, T.; Lindgren, S.-Å.; Olin, H.; Wahlström, E.; Walldén, L. Metal Quantum Wells with All Electrons Confined: Na Films and Islands on Graphite. *Phys. Rev. B* **2001**, *64*, 073301.
(45) An, B.; Zhang, L.; Fukuyama, S.; Yokogawa, K. Growth and Structural Transition of Fe Ultrathin Films on Ni(111) Investigated by LEED and STM. *Phys. Rev. B* **2009**, *79*, 085406.
(46) Mentes, T. M.; Locatelli, A. Angle-Resolved X-ray Photoemission Electron Microscopy. *J. Electron Spectrosc. Relat. Phenom.* **2012**, *185*, 323−329.
(47) Kowalczyk, P. J.; Belić, D.; Mahapatra, O.; Brown, S. A. Grain Boundaries between Bismuth Nanocrystals. *Acta Mater.* **2012**, *60*, 674−681.
(48) Lu, Y. H.; Xu, W. T.; Zeng, M. G.; Yao, G. G.; Shen, L.; Yang, M.; Luo, Z. Y.; Pan, F.; Wu, K.; Das, T.; He, P.; Jiang, J. Z.; Martin, J.; Feng, Y. P.; Lin, Hsin; Wang, X.-S. Topological Properties Determined by Atomic Buckling in Self-Assembled Untrathin Bi(110). *Nano Lett.* **2015**, *15*, 80−87.
(49) Smith, C. G. Low-Dimensional Quantum Devices. *Rep. Prog. Phys.* **1996**, *59*, 235282.
(50) Bian, G.; Wang, X.; Miller, T.; Chiang, T.-C.; Kowalczyk, P. J.; Mahapatra, O.; Brown, A. Firt-Principles and Spectroscopic Studies of Bi(110) Films: Thickness-Dependent Dirac Modes and Property Oscillations. *Phys. Rev. B* **2014**, *90*, 195409.

DOI: 10.1021/acsami.5b00264
ACS Appl. Mater. Interfaces 2015, 7, 8525−8532

(51) Wagner, C. D.; Riggs, W. M.; Davis, L. E.; Moulder, J. F.; Muilenberg, G. E. *Handbook of X-ray Photoelectron Spectroscopy*; Perkin-Elmer Publications: Minnesota, USA, 1979.
(52) Balog, R.; Andersen, M.; Jørgensen, B.; Sljivancanin, Z.; Hammer, B.; Baraldi, A.; Larciprete, R.; Hofmann, P.; Hornekær, L.; Lizzit, S. Controlling Hydrogenation of Graphene on Ir(111). *ACS Nano* **2013**, *7*, 3823−3832.

DOI: 10.1021/acsami.5b00264
ACS Appl. Mater. Interfaces 2015, 7, 8525−8532